Anais XIV Simpósio Brasileiro de Sensoriamento Remoto, Natal, Brasil, 25-30 abril 2009, INPE, p. 2935-2942.

Biogeography of C_3 and C_4 vegetation in South America

Rebecca L. Powell [1]
Christopher J. Still [2]

[1] University of Denver
2050 E. Iliff Ave., Denver, CO 80208, U.S.A.
rpowell8@du.edu

[2] University of California, Santa Barbara
Santa Barbara, CA 93106-4060, U.S.A.l
still@icess.ucsb.edu

Abstract. The C_3/C_4 composition of vegetation is required for a diverse set of carbon cycle research, including inversion studies that use global CO_2 and $\delta^{13}C$ atmospheric data, as well as work that requires the carbon isotope composition of biomass burning emissions. Here, we present continental maps of the abundance and distribution of C_3 and C_4 vegetation for South America. Our approach relies upon the near-universal restriction of C_4 photosynthesis to the herbaceous growth form and the differing performance of C_3 and C_4 plants in various temperature and radiation regimes. The MODIS Vegetation Continuous Fields (VCF) product provides detailed information on growth form composition (% tree, % herbaceous, and % bare) for each grid cell; precipitation and temperature variations are derived from station data climatologies; and crop type fractional coverage accounts for managed agro-ecosystems that may violate the natural climate constraints. A major limitation of the MODIS VCF product is that the vegetation layers do not directly correspond to the percent woody and percent herbaceous cover layers that are needed to accurately derive C_3/C_4 composition of vegetation cover. To address this issue, we develop a rules-based algorithm to separate shrubs and true herbaceous cover from the MODIS 'herbaceous' (i.e., non-tree vegetation) layer using the Global Land Cover 2000 dataset for South America. The $\delta^{13}C$ content of vegetation in South America is then estimated based on the C_3/C_4 composition in each land grid cell, assuming constant values of -27‰ and -12‰ for C_3 and C_4 plant biomass, respectively.

Keywords: remote sensing, C_4 photosynthesis, biogeography, stable isotopes, MODIS continuous fields

1. Introduction

The photosynthetic pathway composition (C_3/C_4 fraction) of vegetation is a fundamental physiological and ecological distinction in tropical and subtropical savannas, as well as in many temperate grasslands. C_4 plants have higher photosynthetic rates at high temperatures and under high light conditions (Collatz et al. 1992) and higher water-use efficiency than do comparable C_3 plants (Sage and Monson 1999). The C_4 photosynthetic pathway occurs predominantly in grasses and in general, C_4 grasses out-compete C_3 plants in high-temperature, lower-moisture environments. For a given CO_2 concentration, the threshold temperature at which C_4 grasses out-compete C_3 grasses is known as the 'crossover temperature' (Ehleringer et al. 1997, Collatz et al. 1998).

The crossover temperature can be used to classify land grid cells as favorable to C_3 or C_4 plants based on climate data (Still et al. 2003), producing a 'climatic theoretical maximum' area of C_4 productivity, which is used as a baseline for establishing the total potential geographical area populated by C_4 plants. The distribution of C_4 plants is then estimated by identifying the abundance of herbaceous vegetation located in the area climatically favorable to C_4 plants (Still et al. 2003). However, to accurately represent the C_3 and C_4 vegetation fraction, the percentage of C_3 and C_4 crops must be incorporated, as the planting of crop types does not always follow the climate rules used to predict C_3 and C_4 dominance in natural grasslands. For example, C_4 corn is one of the top three agricultural crops in the world (Leff et al. 2004), but is often planted in C_3 climate zones; conversely, C_3 crops such as soy can be planted in areas that once were covered by C_4 grasslands.

2. Methods

The C_3/C_4 composition of vegetation was predicted following the methodology developed by Still et al. (2003), but using next generation, finer resolution vegetation cover fraction (VCF) fields, a different climate dataset, and an updated dataset of crop distributions. The algorithm first identifies potential C_4 vegetation cover by identifying herbaceous vegetation that is located in the C_4 climate zone; all other vegetation (i.e., woody vegetation in the C_4 climate zone and all vegetation in the C_3 climate zone) is assumed to utilize the C_3 photosynthetic pathway. The algorithm then integrates data on crop type fractional coverage to account for managed agro-ecosystems that may violate the natural climate constraints. Finally, the $\delta^{13}C$ content of vegetation is estimated from the relative abundance of C_3 and C_4 vegetation in each land grid cell. The algorithm we applied is summarized in Figure 1 and detailed below.

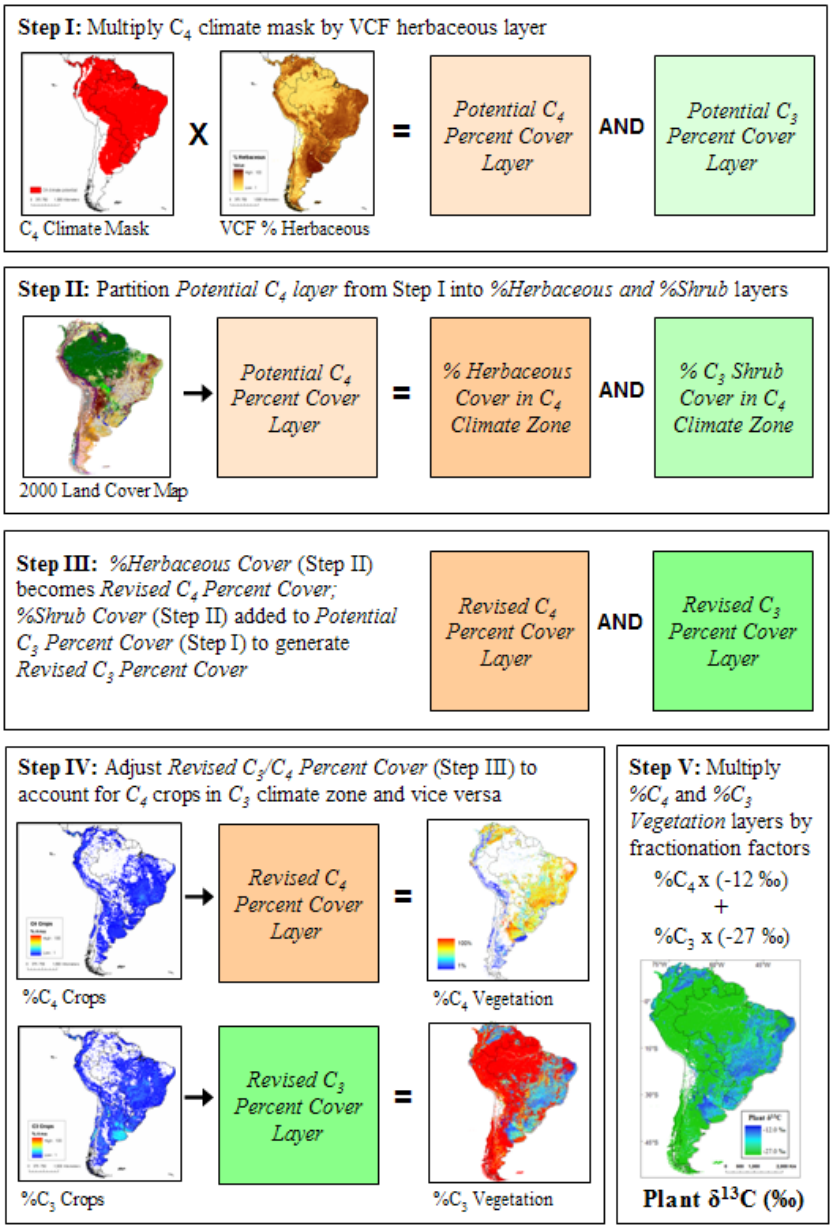

Figure 1. Algorithm to predict plant C_3/C_4 composition and $\delta^{13}C$ (‰) content.

A climate mask of regions considered favorable to C_4 vegetation was generated from a 30-year (1961-1990) mean monthly terrestrial climatology (New et al. 1999, 2000). Each half-degree grid cell that satisfied the two C_4 bioclimatic constraints (mean monthly temperature $\geq 22°$ C and mean monthly precipitation > 25 mm) for at least one month of the year is presented in the upper left corner of Figure 1. Many grid cells satisfied these climate constraints for more than one month.

Vegetation growth-form fields were taken from the MODIS Vegetation Continuous Fields (VCF) product for the year 2001 (Hansen et al. 2003a). The VCF product contains mean annual estimates of the percent cover of herbaceous, tree, and bare soil in each 500-m grid cell. We aggregated the VCF data to 1-km resolution, and all further processing was conducted at this resolution. The MODIS VCF percent herbaceous layer was multiplied by the C_4 climate mask to generate a *Potential C_4 Percent Cover* layer. All other vegetation was assumed to be *Potential C_3 Percent Cover* (Figure 1, Step I).

The MODIS VCF vegetation products correspond to tree and non-tree vegetation layers, rather than the percent woody and percent herbaceous cover layers that are needed to accurately derive percent C_3 and percent C_4 vegetation cover. Specifically, the MODIS VCF percent tree layer represents the percent canopy cover per pixel, i.e., the amount of skylight obstructed by tree canopies, rather than the percent crown cover (Hansen et al. 2003b). The impact of this subtle distinction is twofold. First, the per-pixel percent tree crown *cover* is on average under-estimated. Second, perhaps more importantly, the VCF percent herbaceous layer includes *all* vegetation below 5 m in height (Hansen et al. 2003b), meaning that the 'herbaceous' layer also includes most woody shrubs.

In an attempt to address these issues, the *Potential C_4 Percent Cover* layer was partitioned into shrub and herbaceous layers using the 1-km Global Land Cover (GLC) Map 2000 (Eva et al. 2002; Figure 1, Step II). We identified each GLC land-cover classes as shrub/tree-dominated or grass-dominated, based on the description provided in the dataset documentation (Eva et al. 2002). For pixels assigned to GLC classes consisting predominantly of shrub and tree cover (e.g., 'closed evergreen tropical forest'), the corresponding *Potential C_4 Percent Cover* value was reassigned to the shrub percent cover layer. For pixels assigned to GLC classes dominated by herbaceous cover (e.g., 'grassland savannah' or 'closed steppe grasslands'), the corresponding *Potential C_4 Percent Cover* value was retained as herbaceous percent cover. A few classes were identified as a mix of shrubs and grasses; for these classes, the VCF 'herbaceous' layer was partitioned evenly between the shrub and new herbaceous layer (e.g., 'periodically flooded savannah'). The shrub layer (i.e., what was removed from the original VCF 'herbaceous' layer) was added to the *Potential C_3 Percent Cover* layer, resulting in a *Revised C_3 Percent Cover* layer. The herbaceous cover in C_4 climates that remained after partitioning became the *Revised C_4 Percent Cover* layer (Figure 1, Step III).

The distributions of herbaceous C_3 and C_4 crops were generated from a global dataset of 18 major crop types (Leff et al. 2004), which characterizes the global geographic distribution of crop types using a combination of satellite data and agricultural census data. The C_4 crops in this dataset (corn, sorghum, millet, and sugar cane) were used to calculate the C_4 crop fraction (i.e., fraction of crop area that is C_4) for each grid cell; all other (C_3) crops were used to calculate the C_3 crop fraction. Subsequently, the *Revised C_3* and *Revised C_4 Percent Cover* layers were adjusted to account for C_3 crops planted in the C_4 climate zone and C_4 crops planted in the C_3 climate zone (Figure 1, Step IV). This resulted in *Final C_3* and *C_4 Percent Cover* layers.

The *C_3* and *C_4 Percent Cover* layers were converted to *C_3* and *C_4 Percent Vegetation* layers (i.e., the percent of the vegetation in a given grid cell using either the C_3 or C_4

photosynthetic pathway; this is different from the percentage cover of each pathway in a grid cell when the percent cover of bare soil is non-zero), so that each 1-km grid cell was assigned the proportion of vegetation associated with each photosynthetic pathway (Figure 1, Step IV). That is, sparsely vegetated areas may have low total vegetation cover, yet can have a large C_4 vegetation fraction. The distribution of vegetation stable carbon content ($\delta^{13}C$) was estimated from the *C_3* and *C_4 Percent Vegetation* layers, assuming constant values of -27‰ and -12‰ for C_3 and C_4 organic matter, respectively (Figure 1, Step V).

3. Results and Discussion

The predicted distribution for the C_4 photosynthetic pathway is presented in Figure 2. Comparison of Figure 2a and 2b highlights the difference in predicted C_4 percentages before and after applying the shrub correction; the potential over-estimation of C_4 percentage cover in the original data (Figure 2b) is dramatic. C_4 vegetation is relatively high in the savanna and grassland regions of the continent, particularly in the *cerrado* region south and east of the Amazon forest, the *llanos* in northern Venezuela and Colombia, portions of the *caatinga* in northeast Brazil, and the *pampas* of Argentina and Uruguay. C_3 vegetation cover is greatest in the lowland moist tropical forests of the Amazon Basin, as well as in cooler regions of the continent, such as high-elevation regions of the Andes and low-latitude regions of Patagonia (Figure 3c).

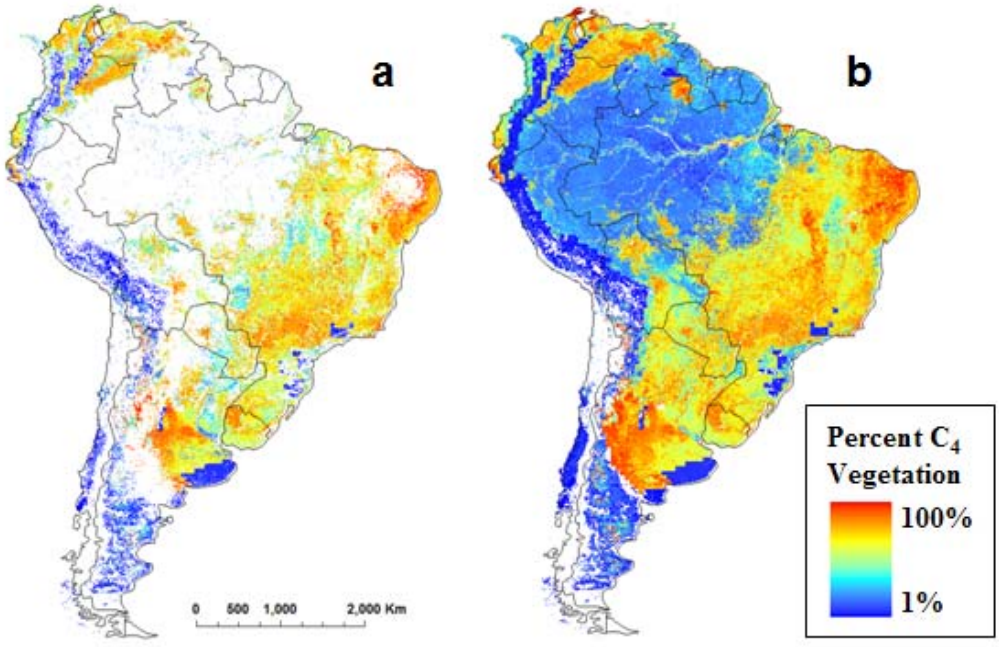

Figure 2. (a) C_4 percent of vegetation with land-cover correction to partition shrubs and herbaceous cover. (b) C_4 percent of vegetation produced using the MODIS VCF herbaceous layer without land-cover correction. Both images have been corrected for crops.

The total area of South America covered by C_3 vegetation is predicted to be approximately 12.1 million km^2, or 69.2% of the total dry land surface, while the total area covered by C_4 vegetation is 3.6 million km^2, or 20.3% or the land surface (Table 1). The remainder of the land surface (approximately 10.5% of the total area) is un-vegetated.

Table 1. Summary of C_3 and C_4 vegetation cover for South America. Areal measurements include dry land surface only. These data are derived from the land-cover and crop-corrected layers.

	Area (10^6 km^2)	**Woody cover** (% area)	**Herb cover** (% area)	**C_3 vegetation** (10^6 km^2)	**C_4 vegetation** (10^6 km^2)	**C_3 vegetation (% area)**	**C_4 vegetation (% area)**
South America	17.6	63.1%	26.4%	12.1	3.6	69.2%	20.3%

The impact of each adjustment made to the VCF percent herbaceous layer (Figure 1, Steps II-IV) on the final predicted C_3 and C_4 vegetation cover is quantified in Table 2. If no adjustment is made to account for crop types planted outside of their climatic zone ('No Corrections' versus 'Crop correction only' in Table 2), the total areal estimates for C_3 and C_4 vegetation cover vary by approximately 0.5% of the total land-surface area. However, if the percent herbaceous layer is not adjusted to account for the presence of shrubs and other low-stature (< 5-m height) woody vegetation, the predicted area of C_3 and C_4 vegetation shifts dramatically ('Land-Cover Correction only' versus 'No Correction' in Table 2). If no land-cover correction is applied to the herbaceous layer, the land area of South America that is covered by C_3 vegetation is only slightly greater than the area covered by C_4 vegetation (48.1% compared to 41.2% of land surface area). When the land-cover correction is applied to the herbaceous layer, the area covered by C_3 vegetation is approximately three times greater than the area covered by C_4 vegetation. Thus, accounting for the distribution of agricultural crops has a relatively small effect on the predicted distribution of C_3 and C_4 vegetation on a continental scale, but failing to account for shrubs and other woody vegetation in the percent 'herbaceous' layer of the VCF product results in a gross overestimation of herbaceous land cover, and in turn, of C_4 vegetation cover.

Table 2. Summary of 'corrections' applied to predict C_3/C_4 vegetation percentages.

	C_3 vegetation (10^6 km^2)	**C_4 vegetation** (10^6 km^2)	**C_3 vegetation (% area)**	**C_4 vegetation (% area)**
No Corrections	8.4	7.2	48.1%	41.2%
Crop correction only	9.0	6.7	51.1%	38.2%
Land-cover correction only	11.8	3.9	67.2%	22.4%
Land-cover and Crop corrections	12.2	3.6	69.2%	20.3%

The spatial patterns of the vegetation stable carbon content ($\delta^{13}C$) directly follow from the C_3/C_4 patterns (Figure 3). The mean predicted $\delta^{13}C$ value for all of South America is -23.7‰. While the algorithm applied to predict the distribution of C_4 vegetation relied on a temperature threshold to sort C_3/C_4 vegetation, regional precipitation gradients also impact the relative abundance of each photosynthetic pathway and thus of vegetation $\delta^{13}C$ composition.

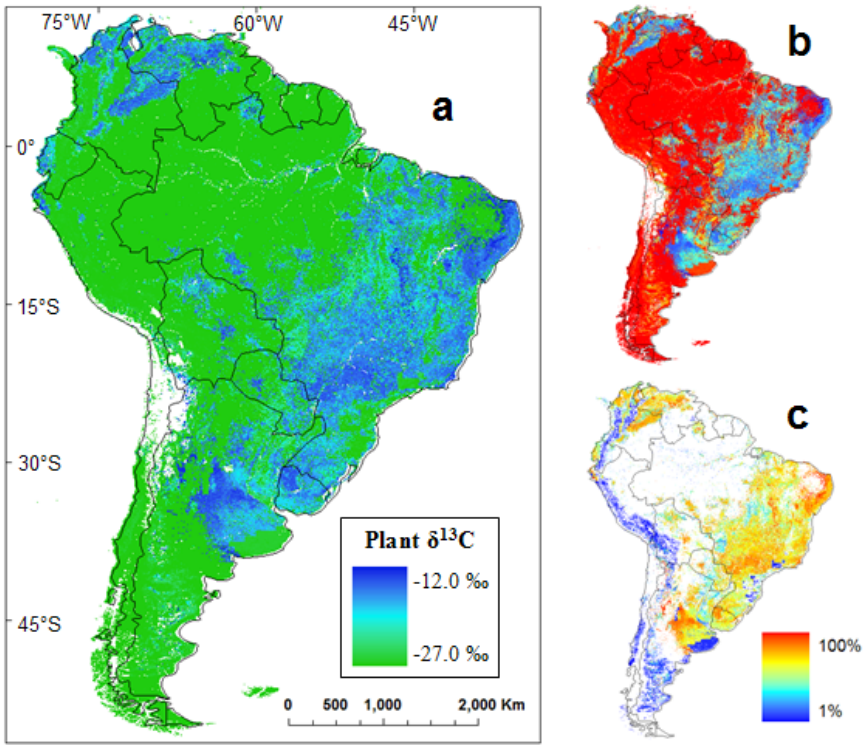

Figure 3. (a) Stable carbon isotopic distribution for the South American continent, (b) percentage of vegetation that uses the C_3 pathway, and (c) percentage of vegetation that uses the C_4 pathway.

At present, there is no way to directly derive the stable carbon composition of vegetation from remotely sensed imagery, and efforts to link remotely sensed parameters to plant $\delta^{13}C$ content remain preliminary but promising (Wang et al., in review). Our methodology therefore relies on the integration of numerous datasets based on the functional and structural characteristics of C_3 and C_4 plants. Each dataset included in our analysis has a different spatial resolution, and each dataset is associated with its own set of errors. We have not attempted to quantify the propagation of error associated with integrating multiple datasets; however, we have highlighted a major source of uncertainty: the estimation of herbaceous vegetation cover.

Because the 'herbaceous' layer of the VCF dataset is more aptly described as a 'non-tree' layer, it must be adjusted to predict the distribution of C_3 and C_4 vegetation. Partitioning the VCF 'herbaceous' layer into 'woody' (i.e., shrub) and true 'herbaceous' (i.e., grasses and forbs) life forms inherently introduces some uncertainty. While the adjustment that we applied to the VCF 'herbaceous' layer probably resulted in an underestimation of herbaceous cover in some biomes of South America, the 'corrected' herbaceous layer more accurately accounts for the true herbaceous distribution than the original VCF data. While the land-cover correction that we applied is a relatively coarse adjustment, it illustrates the limitations of the VCF product if the goal is to discriminate between *woody* and *herbaceous* vegetation cover. Despite the uncertainties introduced, the current version of our product can provide insights into regional patterns of C_3/C_4 distribution and, in turn, the $\delta^{13}C$ composition of vegetation.

Future improvements to this product would ideally generate C_3/C_4 and $\delta^{13}C$ layers that could be used as a much finer spatial scale than the current version. Such improvements would ideally derive new vegetation layers that explicitly map herbaceous and woody life forms, thereby optimizing these data layers for the purpose of mapping C_3/C_4 vegetation; this would eliminate the current land-cover correction step to account for shrubs (Figure 1, Step II). In addition, future studies should investigate the potential of preliminary work that predicts the relative composition of C_3/C_4 vegetation (Foody and Dash 2007) or that predicts the $\delta^{13}C$ content of vegetation directly (Wang et al., in review) based on quantitative relationships between those variables and parameters derived directly from remote sensing imagery.

4. Conclusions

Continental maps of the abundance and distribution of C_3 and C_4 plants provide a first step in improving our understanding of the contribution of C_4 photosynthesis to the global carbon cycle. At present, very little is understood concerning the contribution of C_4 vegetation to interannual terrestrial carbon fluxes. Because C_4 plants are found in regions subject to large climate variability, frequent fires, and intensive agricultural activity, interannual flux variations are expected to be large. Continental-scale maps of vegetation $\delta^{13}C$ content are also useful for a variety of carbon cycle applications, such as predicting the $\delta^{13}C$ composition of emissions from biomass burning (Randerson et al. 2005).

C_4 plants will likely respond quite differently than C_3 plants to the suite of anthropogenic changes being imposed on the earth system, and this will strongly influence C_3/C_4 distributions and terrestrial carbon fluxes. Most directly, land-use/cover changes may exchange one pathway with another; for example, cutting a C_3 tropical forest and replacing it with C_4 pasture grasses, or changing rangeland management practices that lead to the invasion of C_3 shrubs in formerly C_4-dominated savannahs. C_3 and C_4 plants are also expected to respond differently to global climate change. Warmer temperature will generally favor C_4 grasses, while higher atmospheric CO_2 levels will favor C_3 grasses. Finally, change in the timing of precipitation is expected to be an important factor influencing the competitive advantage of C_3 versus C_4 grasses.

Acknowledgements

This work was supported by a NASA New Investigator Program award to CJS. Portions of the methodology were adapted from a manuscript that has been submitted for publication: Still, C. J. and Powell, R. L.. Continental-scale distributions of plant stable carbon isotopes. In: West, J., Bowen, G., Dawson, T., and Tu, K. (Eds.), **Isoscapes: Understanding movement, pattern, and process on Earth through isotope mapping**. Springer, *in review*.

References

Collatz, G. J.; Ribas-Carbo, M.; Berry, J. A. Coupled photosynthesis-stomatal conductance model for leaves of C4 plants. **Australian Journal of Plant Physiology**, v. 19, p. 519-538, 1992.

Collatz, G.J.; Berry, J.A.; Clark, J.S. Effects of climate and atmospheric CO_2 partial pressure on the global distribution of C_4 grasses: present, past, and future. **Oecologia,** v. 114, p. 441-454, 1998.

Ehleringer J.R.; Cerling, T.E.; Helliker, B.R. C-4 photosynthesis, atmospheric CO_2, and climate. **Oecologia**, v. 112, p. 285-299, 1997.

Eva, H. D.; de Miranda, E. E.; Di Bella, C. M.; et al. **A vegetation map of South America**. Luxembourg: Office for Official Publications of the European Commission, 2002. 34 p. (EUR 20159 EN).

Foody, G.M.; Dash, J. Discriminating and mapping the C3 and C4 composition of grasslands in the northern Great Plains, USA**. Ecological Informatics,** v. 2, p. 89-93, 2007.

Hansen, M.; DeFries, R; Townshed, J.R.; Carroll, M; Dimiceli, C.; Sohlberg, R. **Vegetation Continuous Fields MOD 44B, 2001 Percent Tree Cover, Collection 3**, University of Maryland, College Park, Maryland, 2003a.

Hansen, M.C.; DeFries, R.S.; Townshend, J.R.G. et al. Global percent tree cover at a spatial resolution of 500 meters: first results of the MODIS vegetation continuous fields algorithm. **Earth Interactions,** 7: Paper No. 10, 2003b.

Leff, B.; Ramankutty, N.; Foley J. A. Geographic distribution of major crops across the world. **Global Biogeochemical Cycles**, v. 18, GB1009. doi:10.1029/2003GB002108, 2004.

New, M.; Hulme, M., Jones, P. Representing twentieth-century space-time climate variability. Part I: Development of a 1961-90 mean monthly terrestrial climatology. **Journal of Climatology**, v. 12, p. 829-856, 1999.

New, M; Hulme, M; Jones, P. Representing twentieth-century space-time climate variability. Part II: Development of 1901-1996 monthly grids of terrestrial surface climate. **Journal of Climatology**, v. 13, p. 2217-2238, 2000.

Randerson, J.T.; van der Werf, G.R.; Collatz, G.J. et al. Fire emissions from C3 and C4 vegetation and their influence on interannual variability of atmospheric CO2 and d13CO2. **Global Biogeochemical Cycles**, v. 19, p. GB2019, doi:10.1029/2004GB002366, 2005.

Sage, R.F.; Monson, R.K. (Eds.) **C_4 plant biology**. New York: Academic Press, 1999. 596 p.

Still, C.J.; Berry, J.A.; Collatz, G.J.; DeFries, R.S. The global distribution of C_3 and C_4 vegetation: carbon cycle implications. **Global Biogeochemical Cycles**, v. 17, p. GB1006, 2003.

Wang, L.; Okin, G.; Macko, S. Remote sensing of nitrogen and carbon isotope compositions in terrestrial ecosystems. In: West, J., Bowen, G., Dawson, T., and Tu, K. (Eds.), **Isoscapes: Understanding movement, pattern, and process on Earth through isotope mapping**. Springer, *in review*.